4.2 2-D spectral element simulation of the ground motion for a catastrophic earthquake

(E. Priolo)

4.2.1 *Introduction*

The goal of this study is to estimate the strong ground motion in the municipal area of Catania (Italy) for a catastrophic earthquake scenario. The reference earthquake simulates the $M \cong 7$ event of January 11, 1693. The ground motion is computed solving, numerically, the 2-D full-wave seismic equation through the Chebyshev spectral element method (SPEM). The approach used to model the wavefield should be considered “global” as it allows an accurate description of the medium heterogeneity at several scale lengths, solving simultaneously the source and the radiated full wavefield. Particular emphasis is given to the construction of realistic structural models, including the fine local details near the surface.

Simulations are performed for several sources to account for both a change in source position and orientation, and the finite extension of the fault along its dip. The main result of this study are the synthetic seismograms, the peak ground acceleration (PGA) envelopes, and the response spectra at the surface of four transects across the Catania area. The results are validated through the simulation of a different instrumentally recorded event, namely the $M \cong 5.8$ earthquake, which struck Eastern Sicily on December 13, 1990. This report summarises only the most relevant aspects of the whole study. Further details and the whole list of references can be found in (Priolo, 1999). The results of this study are available by anonymous-ftp at: *eprioloftp.ogs.trieste* (directory: *pub/Catania/SPEM*).

4.2.2 *Details about the model, the source, and computations*

All the information available on the structure of the upper 20 km of the Earth's crust of the study region, in terms of propagation velocities, density, and attenuation has been used to construct the model along the transects shown in Figure 4.2. Data consist of three geological profiles, several pre-interpreted seismic lines, data relative to deep wells, a complete geotechnical survey of the area (Faccioli, 1997), and several studies regarding Eastern Sicily and the area surrounding Catania, in particular. On a regional scale, the main units of the crustal structure are: i) the carbonatic basement of the Hyblean Foreland, ii) the sedimentary formations of the Northern Chain, iii) the volcanic body of Mt. Etna, iv) the Ibleo-Maltese escarpment (IBM) running offshore in the NNW-SSE direction, and, on a smaller scale, v) the Gela-Catania Foredeep, with the sedimentary basin of the Catania Plain. Table 4.1 summarises the parameter values adopted for the main formations in the models.

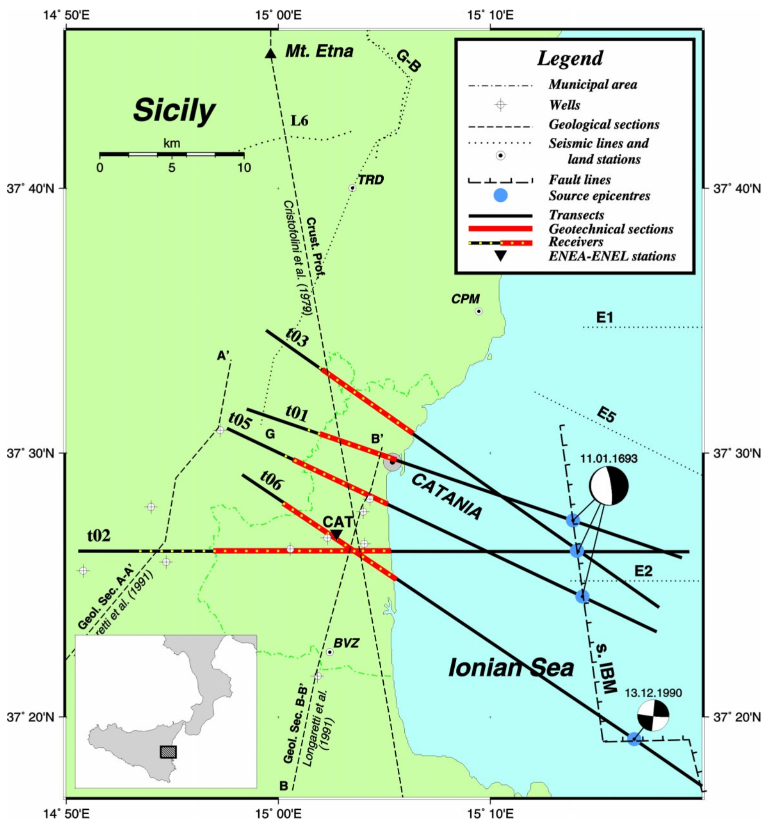

Figure 4.2 - Base map of the study area, showing the essential information about the geography, the transect position, and the data available. The blue circles show the assumed positions of the reference earthquakes of January 11, 1693, and December 13, 1990, respectively.

Table 4.1: Description of the main soil and rock formations used to define the transects. The following parameters are reported: density (ρ)compressional and shear wave velocities (V_P, V_S), and attenuation (Q). The attenuation is computed for a reference frequency of 2 Hz.

Material Description	Id	ρ (km/m^3)	V_P (m/s)	V_S (m/s)	Q (s^{-1})
Clay and silt interbedded with sand	Asg	1950	490	250	12-20
Clay interbedded with sand	Aa	1950-2000	486-950	250-500	15-30
Fine alluvium deposits	Alf	1900	370	190	15
Recent alluvium deposits	Alg	1850	408	210	12
Beach deposits (sands)	M	1830	430	220	12
Filling material, soils, and detrita	R	1800-1900	400-480	210-250	12-15
Sand, coarse gravel and conglomerate	SG	2000	858-875	450	20
Pliocenic sediments and alloctonous	Spa	2000-2150	1400-2800	775-1570	40-100
Scoriaceous and blocky lava flows	X	1800	408	230	15
Lava flows	E	2300	1730	1000	50-100
Vulcanits	V	2580-2630	3900-4100	2250-2335	100-120
Limestone (carbonatic basement)	Cc	2580-2835	4700-7000	2680-3970	120-300

The destructive $M \cong 7$ event of 1693 is commonly associated to rupture with a normal mechanism along the Ibleo-Maltese escarpment. This is a system of sub-vertical normal faults, NNW-SSE oriented, which runs for about 70-100 km offshore along the Ionian coast of Sicily. The reference earthquake of this study is associated to the northern part of the system, which is simplified in a segment about 25 km long (s. IBM in Figure 4.2). Table 4.2 summarises the values of the main source parameters. The source mechanism is of pure normal faulting. The wavefield amplitude is scaled by the value assumed for the fault-slip D.

Table 4.2: Source parameters adopted for the December 11, 1693 earthquake. The following parameters are reported: dimensions of the Ibleo-Maltese northern segment ($L \times W$), source mechanism (strike ϕ, dip δ, and rake λ), magnitude (M), seismic moment (M_0), stress-drop ($\Delta\sigma$), average value of the fault slip (D), and corner frequency (f_C).

$L \times W$ (km)	ϕ (degrees)	δ (degrees)	λ (degrees)	M	M_0 (Nm)	$\Delta\sigma$ (bar)	D (m)	f_C (Hz)
15×25	352	90-65	-90	7	$2\text{-}3 \times 10^{19}$	150	1.2-1.3	0.7

Two groups of sources are considered. The first group used a point source model with the aim of studying the effect induced by a variation in the fault orientation and source position. With the second group, the purpose is to simulate an extended source more closely. To do this, the fault is discretised into three elementary point sources, aligned along the fault dip direction. In this way, three different directions of rupture propagation are reproduced.

The ground motion is predicted along the four transects t02, t05, t01, and t03 (Fig. 4.2). Seismograms are computed up to a maximum frequency of 7.5 Hz and for a total propagation time of 25 s. On average, the size of the computational models is 45 km × 25 km and the meshes contain 170,000-200,000 nodes.

4.2.3 *Discussion*

Figure 4.3 summarises the spatial distribution of PGA predicted for the scenario earthquake. On average, the PGA ranges from between 0.1 and 0.5 g, and, with the exception of a few local peaks, the largest PGA does not exceed 0.7 g. The predicted values do not vary appreciably in the four transects. However, the inability to model ruptures propagating laterally, makes the 2-D methodology applied in this study unsuitable for this kind of conclusions. An unexpected and remarkable feature, which contradicts the classical attenuation trends, is the appreciable increase in PGA for large epicentral distances (i.e.: from 9 km inland in transect t02). As the point source simulations show, the increase is caused by the reflection of a shear wavefront from deep interfaces and occurs only for particular positions of the source with respect to the deep reflectors.

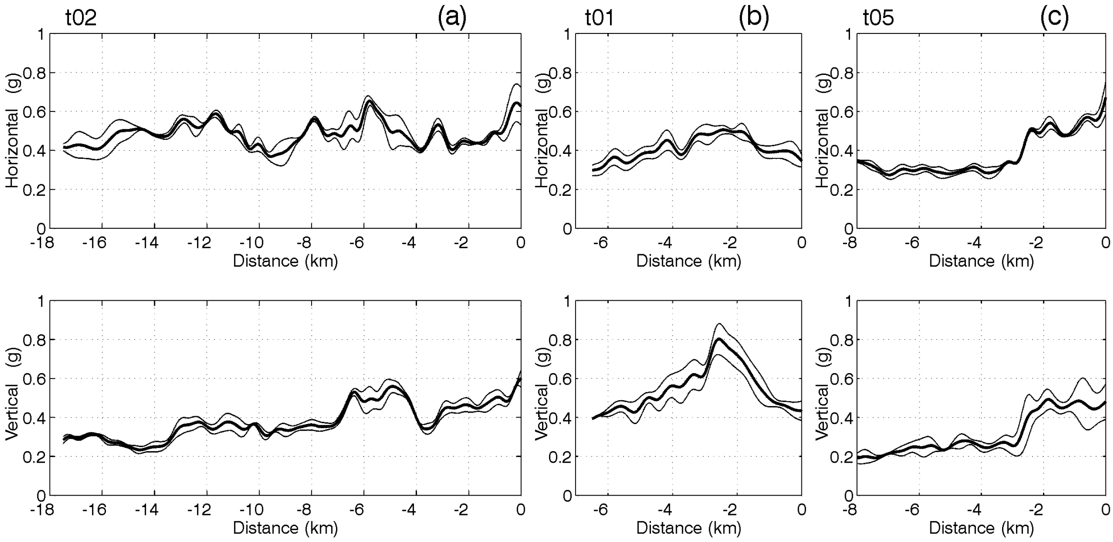

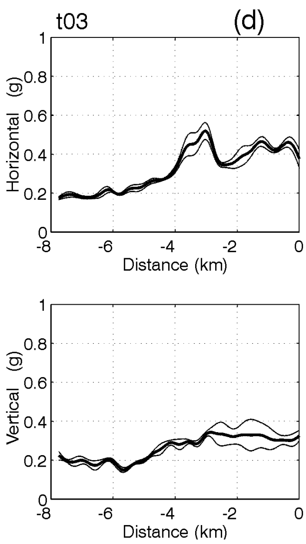

Figure 4.3 - PGA envelopes at the surface of transects (a) t02, (b) t01, (c) t05, and (d) t03, respectively, for the catastrophic earthquake of January 11, 1693. The envelopes are computed for the extended source with three different kinds of rupture propagations. The thick and thin lines represent the mean and the mean plus/minus the first standard deviation, respectively. The average of the two horizontal components (top frames) and the vertical component (bottom) are shown. The abscissa represents the distance from the coastline. Decreasing abscissas correspond to westward direction and increasing epicentral distances. The coastline-epicentre distance (reference epicentres are indicated by blue circles in figure 4.2.1) is 14.5 km for transects t05 and t03, and 13 km for transects t01 and t02, respectively.

Local soil conditions strongly affect the response on a smaller spatial scale, and can change the amplitude dramatically. The ground motion amplitude is always amplified by soft or moderately stiff sediments (e.g.: at 4-6.5 km, 0-2.5 km, 1.5-3 km, and 2.5-4 km in transects t02, t05, t01, and t03, respectively (Fig. 4.3)), and the largest peaks are found, especially, at the transition between lava and sediments. So, seismograms over a lava bed or soft sediments may differ by a factor of two, even at distances of the order of one hundred metres. For sake of brievity here I analyse in more detail the results obtained for only one transect, namely transect t03. The model structure is characterised by two stiff and thick lava banks that cover much of the transect surface (Fig. 4.4a). Horizontal PGA (Fig. 4.3d) features a peak, which exceeds 0.5 g, localised at 2.5-4 km from the coastline, where the soft and low velocity soil outcrops. The anomalous increase of PGA due to the energy reflection at deep crustal interfaces is likely to occur outside the receiver line.

The ground motion can be better analysed looking at the distribution of the response spectra of horizontal acceleration along the surface (Fig. 4.4b). Below 1.5 Hz, the amplitude decays rather smoothly while increasing the epicentral distance, and it has no local anomalies. At higher frequencies, a zone of large amplification – especially in the frequency band 1.5-4 Hz - is predicted at 2.8-3.7 km from the coastline where clay outcrops, and is covered by a thin layer of soft soil. In this zone, we see three almost evenly spaced peaks. The largest peak falls on the transition

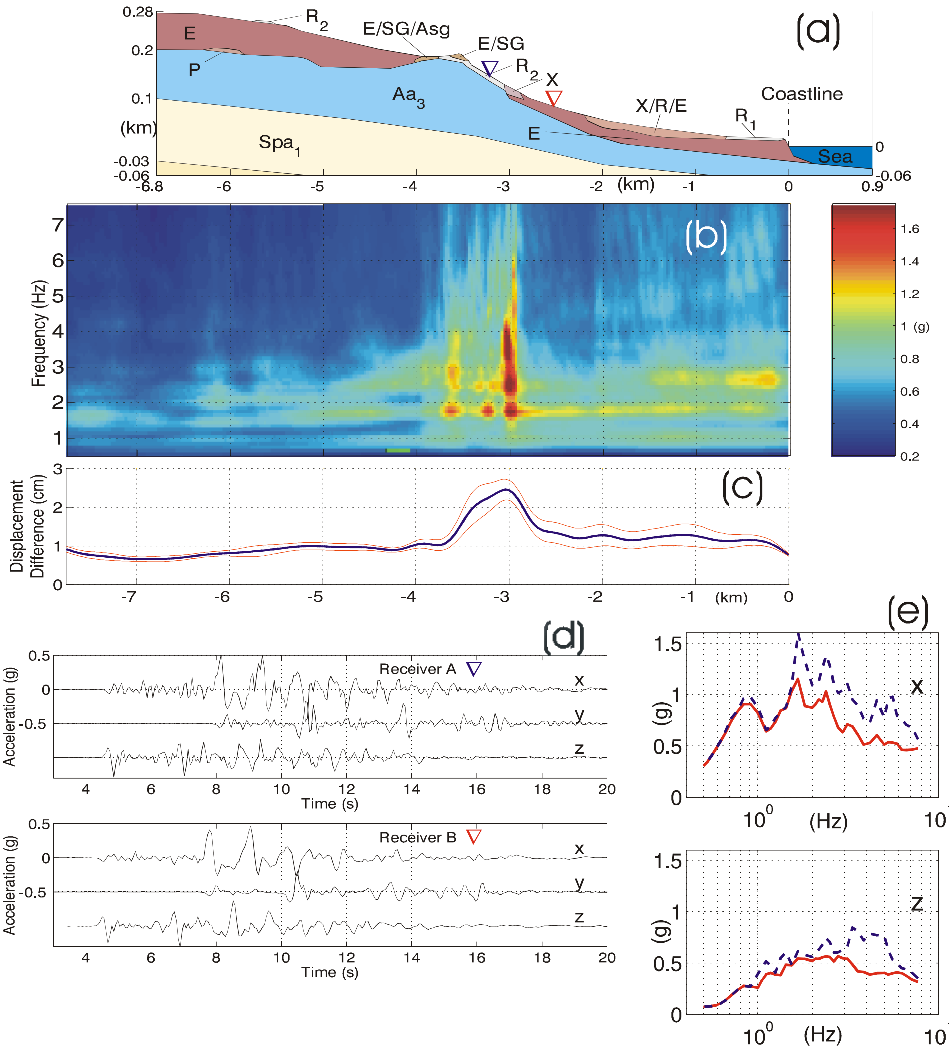

Figure 4.4 - Transect t03. (a) Detail of the uppermost part of the model. See Table 4.1 for the model parameters. Surface distribution of (b) response spectra (5% damping) and (c) displacement difference. Only the horizontal component is displayed. The displacement difference is computed for a receiver distance Δx = 50 m. (d) Seismograms (three components) and (e) response spectra (radial and vertical components) predicted at two near receivers (see panel (a)) located on sediments (A, blue) and lava (B, red), respectively

between stiff/scoriaceous lava to soft soil. Here, the amplification is increased by the irregular geometry of the western edge of the lava bank, which traps energy. Panels (d) and (e) directly compare the ground motion predicted at two near receivers located on lava (receiver B) and on soft soil (A), respectively. Seismograms feature a nearly impulsive response on lava, while a ringing effect and longer coda can be seen in the receiver on soft soil, as a result of the energy, which is trapped within the uppermost layers. The spectra reflect the analysis made above exactly. Compared to the horizontal component, the vertical one features a smaller amplification, which is localised in a higher frequency band (3-5 Hz).

A rather important consideration is that the most potentially significant frequencies for buildings, that is 1.5-4 Hz, are amplified mostly in the horizontal components. They correspond to the natural frequencies of a stack of sediment layers about 30-100 m thick where the average shear-wave velocity is about 500-600 m/s. On the contrary, the very thin surficial layers (e.g.: R_2 in Figure 4.4a), despite the low shear-wave velocity of 200-250 m/s, are too thin to interfere constructively with the exciting wavefield. They just increase the overall amplitude of the signal. As a general conclusion, the thin layers of soft soil, which may be found at the ground surface, produce amplification of the ground motion, but do not affect the signal spectrum. By contrast, the frequencies of interest for civil engineering structures can be selectively enhanced by a thicker portion of surface sediments. A detailed knowledge of the seismic properties of the uppermost layers, down to a depth of about 100-150 m, is therefore of maximum interest for a reliable prediction of the strong ground motion.

Finally, Figure 4.4c shows the maximum displacement difference predicted along the transect surface. This quantity may be important for predicting damage to lifelines and bridges. As expected, the largest values (about 2.5 cm for a distance of 50 m) occur at the transition between lava and soft soil.

4.2.4 *Validation of the methodology*

No records are currently available for earthquakes occurring along the segment of the Malta Escarpment considered in this study. Therefore, the approach is validated by simulating an event which occurred nearby, that is the December 13, 1990 $M \cong 5.8$ Eastern Sicily earthquake. It was recorded by a few stations of the ENEA-ENEL, national accelerometer network (Fig. 4.2), and in particular by the Catania station. The earthquake is associated to rupture of the transcurrent segment of the Ibleo-Maltese fault.

The computational model is defined along transect t06. The structure is consistent with that of the other transects of this study. The source is a point, and the fault mechanism is defined by $(\phi, \delta, \lambda) = (96°, 85°, 180°)$, according to Giardini *et al.* (1995). Corner frequency, source depth, and fault-slip amplitude are set at $f_C = 1.3$ Hz (Di Bona *et al.*, 1995), $z_S = 20$ km (Amato *et al.*, 1995), and $D = 0.7$ m (Somerville *et al.*, 1999), respectively. Seismograms are computed up to a maximum frequency of 6 Hz and for a total propagation time of 40 s.

Figure 4.5 displays seismograms predicted at and recorded by the strong motion Catania station. They compare well in terms of the overall shape, polarity of the main arrivals, S-wave amplitude, and seismogram duration. However, a large amplification of all P-waves is observed in the synthetics (e.g., in the early 4 s). This can be ascribed to the rather low V_P values imposed on the surface soils, which are needed to overcome the inability of the method to deal with materials characterised by large V_P/V_S ratios. Besides, we note here that, even if we adopt a simple point source, the calculated seismograms are quite realistic. This supports the use of methods that accurately model realistic geologic structures.

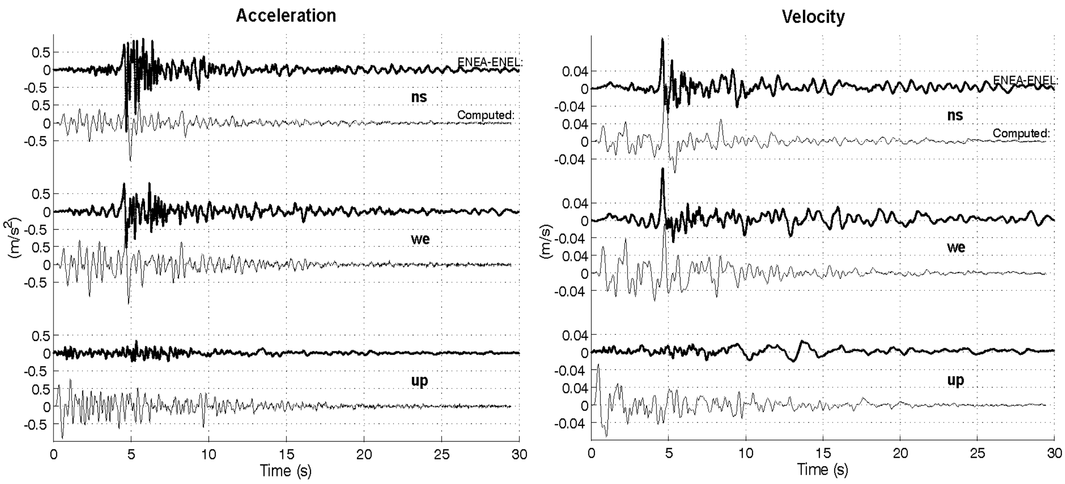

Figure 4.5 - The December 13, 1990, M ≅ 5.8 *Eastern Sicily earthquake. Three component acceleration (left panel) and velocity (right) seismograms recorded by Catania station (thick lines), and those predicted using 2-D spectral element modelling (thin lines). The observed seismograms are band-pass filtered at 0.25-6 Hz, and the velocity is obtained by time integration of the acceleration records. The origin time of predicted seismograms has been aligned to that of the recorded seismograms*

4.2.5 *Measurements of environmental seismic noise for site response prediction*

(E. Priolo and A. Michelini, with the collaboration of E. Faccioli, R. Addia and A. Puglia, M. Mucciarelli and R. Gallipoli)

A survey of environmental seismic noise (microtremors) was carried out within the Catania municipal area in May 1999. The aim of the data acquisition was to improve our local prediction of the seismic ground motion. To this end, we followed Nakamura’s approach. As shown in previous studies, this method provides the main features of the dynamic ground response through the calculation of the spectral ratio between the horizontal and the vertical components (i. e., H/V ratio) of background noise (Nakamura, 1989).

The seismic noise was recorded at 37 different sites (Fig. 4.6). These sites were chosen according to the following criteria: 1) significance in terms of geological, geotechnical, or local characteristics; 2) presence of a lithological transition (e.g.: the transition from lava flows to sediments); 3) presence of other geotechnical or geophysical measures; 4) alignment with some of the transects along which the ground motion had been simulated numerically.

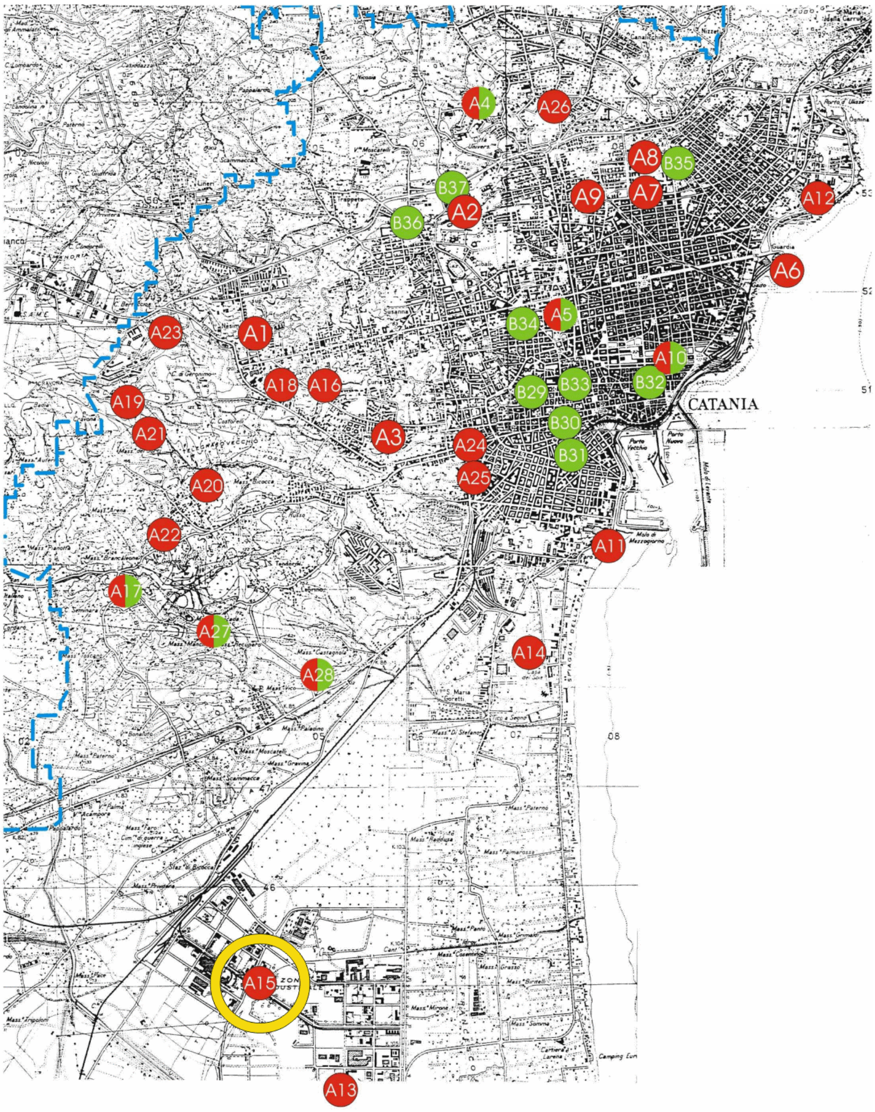

Figure 4.6 – Map of the area. Circles show the sites measured. Red and green colours indicate the measurements performed by the "Nanometrics Orion" portable seismic station and the "Ismes Background-noise analyser", respectively. The ENEA-ENEL accelerometric site is circled in yellow.

All conditions that could affect the quality of the measurements and mask the soil response (e.g.: geophones positioned directly on asphalt paving or very close to buildings) were avoided. The data were acquired by two teams independently. The first team was made up of the authors, and equipped with Orion Nanometrics portable seismic stations (red circles in Fig. 4.6) whereas the second team with M. Mucciarelli and R. Gallipoli, used the “Ismes Background-noise analyser” (green circles). Both instruments were equipped with Lennartz LE-3D/1s seismometers. Simultaneous measurements were performed at eight locations. The recorded noise level was high enough at all sites.

In Figure 4.7, we compare the H/V spectral ratios obtained from i) the seismic noise (the mean value of the ratios obtained from the two measurements taken near the Catania ENEA-ENEL accelerograph site), ii) the signals recorded by the SMA-1 accelerograph during the December 13, 1990 $M = 5.8$ Eastern Sicily earthquake, and iii) the seismograms computed by the 2-D spectral element method for the same earthquake. The ratios obtained from the seismic noise measurements detect well the fundamental mode of vibration at about 1.5 Hz, but they miss the peak at the higher frequency of 4-5 Hz. This fact may either confirm that Nakamura’s method is reliable for identifying only the fundamental mode of vibration, or that the peak at 4-5 Hz in the earthquake records is a feature of the earthquake source. The H/V ratios determined from the synthetic seismograms are generally noisier. Specifically, we see that the ratios obtained from the synthetic seismograms reproduce well the behaviour of the spectral ratios determined from the full accelerograph recordings for frequencies larger than 1 Hz, whereas the origin of the two additional peaks at 0.4-0.8 is currently under investigation. The results of this study will be made available by anonymous-ftp at site: *eprioloftp.ogs.trieste* (directory: *pub/Catania/SeismicNoise*).

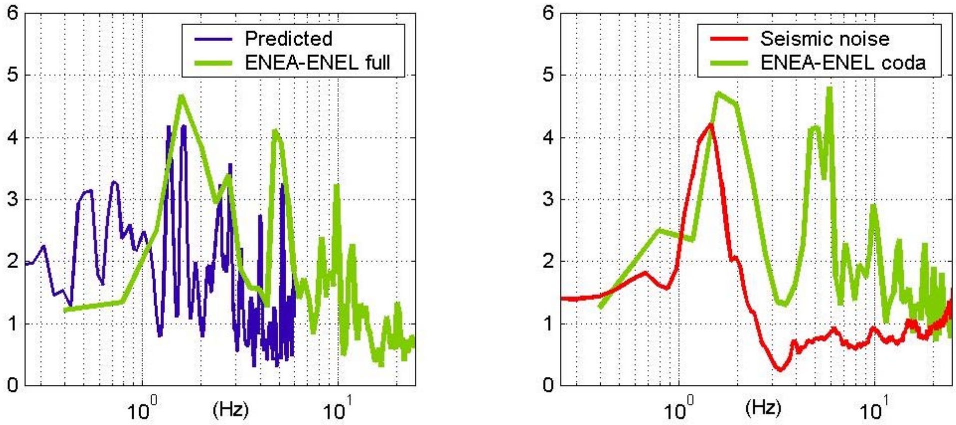

Figure 4.7 – H/V spectral ratios computed for the ENEA-ENEL Catania accelerograph (SMA-1) station. Green curves: ratios determined from the recordings of the December 13, 1990 Eastern Sicily earthquake (full record and coda from 20 to 45 s, left and right panels, respectively). Blue curve: ratios obtained from the modelling of the same event and using the SPEM 2-D spectral element code. Red curve: ratios obtained from the seismic noise measurements.